Calcitonin gene-related peptide alleviates hyperoxia-induced human alveolar cell injury via the CGRPR/TRPV1/Ca^{2+} axis

JUN-HUI LI[1], HAN-XING WAN[1], LI-HONG WU[1], FANG FANG[1], JIAN-XIN WANG[2], HUI DONG[1,2] and FENG XU[1]

[1]Department of Pediatric Intensive Care Unit, Children's Hospital of Chongqing Medical University, National Clinical Research Center for Child Health and Disorders, Ministry of Education Key Laboratory of Child Development and Disorders, Chongqing Key Laboratory of Pediatric Metabolism and Inflammatory Diseases, Chongqing 400037, P.R. China;
[2]Department of Pharmacology, School of Pharmacy, Qingdao University Medical College, Qingdao, Shandong 266073, P.R. China

Received February 20, 2024; Accepted April 12, 2024

DOI: 10.3892/mmr.2024.13234

Abstract. Although exogenous calcitonin gene-related peptide (CGRP) protects against hyperoxia-induced lung injury (HILI), the underlying mechanisms remain unclear. The present study attempted to elucidate the molecular mechanism by which CGRP protects against hyperoxia-induced alveolar cell injury. Human alveolar A549 cells were treated with 95% hyperoxia to establish a hyperoxic cell injury model. ELISA was performed to detect the CGRP secretion. Immunofluorescence, quantitative (q)PCR, and western blotting were used to detect the expression and localization of CGRP receptor (CGRPR) and transient receptor potential vanilloid 1 (TRPV1). Cell counting kit-8 and flow cytometry were used to examine the proliferation and apoptosis of treated cells. Digital calcium imaging and patch clamp were used to analyze the changes in intracellular Ca^{2+} signaling and membrane currents induced by CGRP in A549 cells. The mRNA and protein expression levels of Cyclin D1, proliferating cell nuclear antigen (PCNA), Bcl-2 and Bax were detected by qPCR and western blotting. The expression levels of CGRPR and TRPV1 in A549 cells were significantly downregulated by hyperoxic treatment, but there was no significant difference in CGRP release between cells cultured under normal air and hyperoxic conditions. CGRP promoted cell proliferation and inhibited apoptosis in hyperoxia, but selective inhibitors of CGRPR and TRPV1 channels could effectively attenuate these effects; TRPV1 knockdown also attenuated this effect. CGRP induced Ca^{2+} entry via the TRPV1 channels and enhanced the membrane non-selective currents through TRPV1 channels. The CGRP-induced increase in intracellular Ca^{2+} was reduced by inhibiting the phospholipase C (PLC)/protein kinase C (PKC) pathway. Moreover, PLC and PKC inhibitors attenuated the effects of CGRP in promoting cell proliferation and inhibiting apoptosis. In conclusion, exogenous CGRP acted by inversely regulating the function of TRPV1 channels in alveolar cells. Importantly, CGRP protected alveolar cells from hyperoxia-induced injury via the CGRPR/TRPV1/Ca^{2+} axis, which may be a potential target for the prevention and treatment of the HILI.

Correspondence to: Dr Hui Dong, Department of Pharmacology, School of Pharmacy, Qingdao University Medical College, 1 Ningde Road, Qingdao, Shandong 266073, P.R. China
E-mail: donghui@qdu.edu.cn

Dr Feng Xu, Department of Pediatric Intensive Care Unit, Children's Hospital of Chongqing Medical University, National Clinical Research Center for Child Health and Disorders, Ministry of Education Key Laboratory of Child Development and Disorders, Chongqing Key Laboratory of Pediatric Metabolism and Inflammatory Diseases, 136 Zhongshan Second Road, Chongqing 400037, P.R. China
E-mail: xufeng9899@163.com

Abbreviations: CGRP, calcitonin gene-related peptide; CGRPR, CGRP receptor; GPCR, G protein-coupled receptor; TRPV1, transient receptor potential vanilloid 1; AECII, alveolar type II epithelial cells; HILI, hyperoxia-induced lung injury; PLC, phospholipase C; PKC, protein kinase C

Key words: hyperoxia, A549 cells, TRPV1, proliferation, apoptosis

Introduction

Hyperoxia therapy is often used to treat premature infants and children with acute hypoxic respiratory failure, and although it may improve their survival rate, it can also easily cause acute and chronic lung injury (1,2). Hyperoxia-induced lung injury (HILI) is a common neonatal emergency and a major cause of severe permanent lung injury and death (3,4). However, the exact pathogenesis of HILI remains unclear, thus hindering the development of effective treatments. HILI primarily affects alveolar epithelial cells, especially alveolar type II epithelial cells (AECII), a subgroup that functions as stem cells for growth and damage repair (5). Therefore, it is of significant interest and clinical value to study the regeneration and repair of AECII and to explore the underlying pathological mechanisms of early intervention strategies for HILI.

Calcitonin gene-related peptide (CGRP) is a neuropeptide transmitter that is synthesized primarily by neurons, but AECII can also synthesize CGRP (6-9). CGRP exerts its biological functions by binding to its specific CGRP receptor (CGRPR), which is a G protein-coupled receptor (GPCR) (10). CGRP is not only a potent vasodilator (11), but it is also

involved in the occurrence and development of pain (12,13), inflammation (14,15), cardiovascular disease (16,17) and wound healing (18). It has been reported that CGRP can alleviate lung injury by inhibiting ischemia-reperfusion and lipopolysaccharide-induced inflammation (19-21), but its role in the development and progression of HILI remains unclear. Previous studies by the authors revealed that CGRP plays an important role in repairing damage caused by HILI by inhibiting apoptosis and promoting cell proliferation in AECII (22-25), but the underlying molecular mechanisms are largely unclear. Therefore, further investigations on the role and mechanisms of CGRP in the repair of damage caused by HILI may assist in the development of effective strategies for the prevention and treatment of HILI.

Transient receptor potential vanilloid 1 (TRPV1) is a non-selective cationic channel protein that can be activated by physical and chemical stimuli, such as traction stimulation (for example, lung ventilation) or capsaicin, to facilitate the entry of Ca^{2+}-dominant cations, thus participating in a variety of physiological or pathological processes (26,27). Although several studies have revealed that activation of TRPV1 channels promotes Ca^{2+}-dependent CGRP production and release from sensory endings (28,29), whether CGRP plays a role by inversely regulating TRPV1 channels is unknown, to the best of the authors' knowledge. Furthermore, although TRPV1 channels expressed in lung epithelial cells play a protective role in ischemia-reperfusion injury (19,30), its role in AECII has not been reported, to the best of the authors knowledge, let alone its potential involvement in the pathogenesis of HILI.

Therefore, the aim of the present study was to explore the protective effects of CGRP against HILI and its underlying molecular mechanisms, focusing on its downstream signaling pathway. It was revealed that CGRP exerted a protective role in HILI via a novel and unique CGRPR/TRPV1/Ca^{2+} signaling axis, highlighting a potential target for the prevention and treatment of HILI.

Materials and methods

Cell culture and induction of hyperoxia. Human alveolar A549 cells were purchased from Haixing Biological Technology Co., Ltd. (cat. no. TCH-C116). Cells were cultured in DMEM-HIGH Glucose medium supplemented with 10% fetal bovine serum (AusGeneX Pty Ltd.), 100 U/ml penicillin and 0.1 mg/ml streptomycin (Beyotime Institute of Biotechnology). The cells were plated in 6- or 96-well plates for subsequent experiments. When the cell confluence reached 50-60%, the cells were treated with 10 nM CGRP (cat. no. HY-P1548A; MedChemExpress) or 1 μM capsaicin (cat. no. HY-10448; MedChemExpress), and then stimulated with hyperoxia. Cells were pretreated with $CGRP_{8-37}$ (cat. no. HY-P1014), SB-705498 (cat. no. HY-10633), BAPTA-AM (cat. no. HY-100545), U-73122 (cat. no. HY-13419), U-73343 (cat. no. HY-108630), or Go6976 (cat. no. HY-10183; all from MedChemExpress) for 2 h before CGRP treatment. Hyperoxia exposure was defined as cells cultured in a closed oxygen chamber (Billups-Rothenberg, Inc.) supplied with 95 O_2 and 5% CO_2 for 24 h (31). The cells of the control group were cultured under normal air conditions. All cells were cultured at a constant temperature of 37˚C and supplied with 5% CO_2.

Lentivirus infection. Lentivirus infection was performed as previously described (32). Lentivirus was purchased from OBiO Technology Corp., Ltd. The TRPV1 shRNA and shNC primer sequences are shown in Table I. A549 cells were infected with lentivirus according to the manufacturer's protocol, and stable cells were screened with puromycin 72 h later.

Immunofluorescence assay. A549 cells were plated on 24-well coverslips at a density of $5x10^4$/ml. When the confluence reached 60-70%, the cells were fixed with 4% paraformaldehyde at room temperature for 15 min, and washed with PBS three times. Cells were blocked with 1% bovine serum albumin (Beyotime Institute of Biotechnology) at room temperature for 30 min, then incubated with anti-TRPV1 antibody (1:200; cat. no. ACC-030; Alomone Labs) for 2 h at 4˚C or anti-CGRPR antibody (1:200; cat. no. A8533; ABclonal) overnight at 4˚C. After washing with PBS, cells were incubated with Alexa Fluor 488-labeled anti-rabbit secondary antibody (1:500; cat. no. A0423; Beyotime Institute of Biotechnology) at room temperature for 1 h. Cell nuclei were counterstained with 5 μg/ml DAPI at room temperature for 5 min, and images were captured using a confocal microscope (Nikon Corporation).

Cell counting kit-8 (CCK-8) proliferation assay. Cell proliferation assay was performed as previously described (31,32). Cell proliferation was measured using a CCK-8 assay (cat. no. HY-K0301; MedChemExpress). A549 cells were plated in 96-well plates at a density of $4x10^4$/ml. After 24 h, the media was replaced, the treatments were applied, and cells were cultured in either normal air or hyperoxic conditions for 24 h. Next, 100 μl medium containing 10% CCK-8 solution was added to each well and incubated for 1-2 h at 37˚C. The optical density was measured at 450 nm using a spectrometer. Cell viability was calculated using the absorbance method to express cell proliferation (33).

Apoptosis assay. Apoptosis assay was performed as previously described (31). Apoptosis detection kits were purchased from BD Biosciences (cat. no. 556547) or Shanghai Yeasen Biotechnology Co., Ltd. (cat. no. 40302ES). Cells were plated in 6-well plates for 24 h at 37˚C and then treated with the various drugs for another 24 h. The cells were digested using EDTA-free trypsin for 2 min, transferred to flow tubes, centrifuge at 300 x g for 5 min at room temperature, and washed twice with PBS. Subsequently, cells were resuspended in 100 μl Annexin V Binding Buffer, and 5 μl FITC Annexin V and 5 μl PI were added. Then, the cells were gently rocked and incubated for 15 min in the dark at room temperature, after which, 400 μl Binding Buffer was added to the cell suspension. Apoptosis was measured using a flow cytometer (Beckman Coulter Life, Inc.) and analyzed using FlowJo software (version 10.8.1; FlowJo LLC). Apoptosis cells (%)=Q2 (late apoptotic cells) + Q3 (early apoptotic cells).

Calcium measurement. A549 cells were plated on coverslips and incubated with 5 μM Fura-2 AM (cat. no. F1221; Invitrogen; Thermo Fisher Scientific, Inc.) in physiological salt solution (PSS) at 37˚C for 60 min, then washed with PSS with or without antagonist for 20 min. Cells on coverslips were

Table I. Primer sequences for TRPV1 shRNA in A549 cells.

Gene name	Primer sequence (5'→3')
TRPV1-shRNA-1	F: CCGGCCGTTTCATGTTTGTCTACATCTCGAGATGTAGACAAACATGAAACGGTTTTTTG
	R: AATTCAAAAAACCGTTTCATGTTTGTCTACATCTCGAGATGTAGACAAACATGAAACGG
TRPV1-shRNA-2	F: CCGGGAAGTTTATCTGCGACAGTTTCTCGAGAAACTGTCGCAGATAAACTTCTTTTTTG
	R: AATTCAAAAAAGAAGTTTATCTGCGACAGTTTCTCGAGAAACTGTCGCAGATAAACTTC
TRPV1-shRNA-3	F: CCGGGCGCATCTTCTACTTCAACTTCTCGAGAAGTTGAAGTAGAAGATGCGCTTTTTTG
	R: AATTCAAAAAAGCGCATCTTCTACTTCAACTTCTCGAGAAGTTGAAGTAGAAGATGCGC
TRPV1-shNC	F: CCGGCCTAAGGTTAAGTCGCCCTCGCTCGAGCGAGGGCGACTTAACCTTAGGTTTTTTG
	R: AATTCAAAAAACCTAAGGTTAAGTCGCCCTCGCTCGAGCGAGGGCGACTTAACCTTAGG

TRPV1, transient receptor potential vanilloid 1; F, forward; R, reverse; shRNA, short hairpin RNA; NC, negative control.

then mounted in a standard perfusion chamber on a Nikon microscope table. The fluorescence ratio of Fura-2 (F340/380) was tracked over time at an excitation wavelength of 340 or 380 nm and captured using an intensified CCD camera (Hamamatsu Photonics K.K.) and a MetaFluor Imaging system (Version 7.10.4.407; Molecular Devices, LLC). The ratio of F340/380 represented the intracellular Ca^{2+} levels and was quantified using Δ(F340/380), that is, the difference between the baseline and maximum values after stimulation. The PSS for Ca^{2+} measurement consisted of the following: 140 mM NaCl, 5 mM KCl, 2 mM $CaCl_2$, 10 mM HEPES and 10 mM glucose at pH 7.3. The osmolality of the solution was ~300 mOsmol/kg H_2O.

Electrophysiological recordings. Whole-cell membrane currents of A549 cells were recorded with an EPC 10 USB Double Patch Clamp Amplifier (HEKA). Data were digitized at 10 kHz and filtered at 5 kHz. The cell voltage was fixed at 0 mV to inactivate voltage-gated calcium and sodium channels, and a 100 ms linear ramp protocol (-100 to 100 mV) was applied every 2 sec. The amplitude of the current was recorded. The extracellular buffer contained 140 mM NaCl, 5 mM KCl, 2 mM $CaCl_2$, 2 mM $MgCl_2$ and 10 mM HEPES at pH 7.3. The pipette solution contained 140 mM CsCl, 5 mM EGTA, 3 mM Mg-ATP, and 10 mM HEPES at pH 7.3. The osmolality of all the solutions was ~300 mOsmol/kg H_2O.

Reverse transcription-quantitative PCR (RT-qPCR). RT-qPCR was performed as previously described (34). Total RNA was extracted using an RNA isolation kit (cat. no. R0027; Beyotime Institute of Biotechnology). Then, cDNA synthesis was performed using PrimeScript™ RT MasterMix (cat. no. RR036A; Takara Bio, Inc.) according to the manufacturer's instructions. Finally, using 1,000 ng cDNA as the template, SYBR Green qPCR MasterMix (cat. no. HY-K0523; MedChemExpress) was added in a 10 μl reaction system for qPCR. The amplification procedure was as follows: Heating at 95˚C for 5 min to activate the hot-start DNA polymerase, followed by 40 cycles of 10 sec at 95˚C and 30 sec at 60˚C. The data were quantified using the $2^{-\Delta\Delta Cq}$ relative quantification method (35), and β-actin was used as the internal control. The primers were designed and purchased from Sangon Biotech Co., Ltd. The primer sequences are shown in Table II.

Table II. Primer sequences for quantitative PCR.

Gene name	Primer sequence (5'→3')
CGRPR	F: ATGGAGAAAAAGTGTACCCTGT
	R: TGAATGGGGTCTTGCATAATCT
TRPV1	F: TGGTATTCTCCCTGGCCTTG
	R: CTTCCCGTCTTCAATCAGCG
Cyclin D1	F: GTCCTACTTCAAATGTGTGCAG
	R: GGGATGGTCTCCTTCATCTTAG
PCNA	F: TAATTTCCTGTGCAAAAGACGG
	R: AAGAAGTTCAGGTACCTCAGTG
Bcl-2	F: GACTTCGCCGAGATGTCCAG
	R: GAACTCAAAGAAGGCCACAATC
Bax	F: CGAACTGGACAGTAACATGGAG
	R: CAGTTTGCTGGCAAAGTAGAAA
β-actin	F: CCTGGCACCCAGCACAAT
	R: GGGCCGGACTCGTCATAC

CGRPR, CGRP receptor; TRPV1, transient receptor potential vanilloid 1; F, forward; R, reverse; PCNA, proliferating cell nuclear antigen.

Western blotting. RIPA Lysis Buffer (cat. no. HY-K1001; MedChemExpress) containing 1% protease inhibitor cocktail (cat. no. HY-K0010; MedChemExpress), 1% phosphatase inhibitor cocktail (cat. no. HY-K0021; MedChemExpress) and 1% PMSF Solution (cat. no. ST507; Beyotime Institute of Biotechnology) was used to extract proteins from the pretreated cells. The protein concentration was determined using a bicinchoninic acid assay (cat. no. P0010; Beyotime Institute of Biotechnology), and then the total protein was mixed with SDS-PAGE loading buffer and boiled for 10 min. Equal amounts of 30 μg protein were loaded on a 10% SDS-PAGE gel (cat. no. PG112; EpiZyme, Inc.) for electrophoretic separation, and transferred to PVDF membranes (cat. no. ISEQ00010; MilliporeSigma). Blots were blocked for 10 min at room temperature using rapid blot blocking buffer (cat. no. P30500; New Cell & Molecular Biotech Co., Ltd.), and then incubated at 4˚C overnight with the following specific primary antibodies:

anti-TRPV1 (1:500), anti-CGRPR (1:500), anti-PCNA (1:1,000; cat. no. 13110; Cell Signaling Technology, Inc.), anti-Cyclin D1 (1:1,000; cat. no. 55506; Cell Signaling Technology, Inc.), anti-Bcl-2 (1:1,000; cat. no. 60178-1-Ig, ProteinTech Group, Inc.), anti-Bax (1:5,000; cat. no. 60267-1-Ig; ProteinTech Group, Inc.), anti-β-actin (1:1,000; cat. no. 4970; Cell Signaling Technology, Inc.), or anti-GAPDH (1:1,000; cat. no. 2118; Cell Signaling Technology, Inc.).

After the primary antibody was recovered, TBST (0.05% Tween-20) was used to wash the membrane three times, 8 min each time. Then the membranes were incubated with goat anti-rabbit (cat. no. ZB-2301) or goat anti-mouse (cat. no. ZB-2305; ZSGB Biotechnology, Inc.) secondary antibody for 1 h at room temperature. The dilution ratio of the secondary antibodies was 1:5,000. Signals were visualized using enhanced chemiluminescence reagent (MilliporeSigma) and densitometric analysis was performed using ImageJ software (version Fiji; National Institutes of Health).

ELISA. ELISA was performed as previously described (34). The levels of CGRP in the supernatant of A549 cells treated with air or hyperoxia were detected using a human CGRP ELISA kit (cat. no. CB-E08210h; Cusabio Technology, LLC) according to the manufacturer's protocol.

Statistical analysis. SPSS version 25.0 (IBM Corp.) was used to analyze the data. All data are presented as the mean ± SD of at least three repeats. The unpaired Student's t-test was used for comparison between two groups. A one-way ANOVA was used for comparison among multiple groups; if the variances were homogeneous, a Fisher's least significant difference test was used for analysis; otherwise, Dunnett's T3 analysis was used. $P<0.05$ was considered to indicate a statistically significant difference.

Results

Hyperoxia downregulates CGRPR and TRPV1 channels expression in A549 cells. Since CGRP exerts its biological effects by binding to its specific CGRPR (10), to confirm whether CGRP exerted its protective effects through TRPV1, immunofluorescence was first performed to detect the expression and localization of CGRPR and TRPV1 in A549 cells. CGRPR and TRPV1 were expressed and were primarily located in the cytoplasm and cell membrane (Fig. 1A). Whether hyperoxia affects CGRP release is unknown, thus, A549 cells were cultured either in normal air or hyperoxic conditions, after which, the release of CGRP was detected. ELISA results revealed that there was no difference in CGRP release between the air and hyperoxia groups (Fig. 1B). At the same time, the effect of hyperoxia on the expression of CGRPR and TRPV1 channels in A549 cells was examined. After incubation under hyperoxic conditions, the mRNA and protein expression levels of CGRPR were significantly decreased compared with cells cultured with normal air (Fig. 1C and D). Similarly, the mRNA and protein expression levels of TRPV1 were also considerably reduced (Fig. 1E and F). Therefore, these results showed that hyperoxia downregulates the expression of CGRPR and TRPV1 channels in A549 cells without altering CGRP release.

CGRP/CGRPR and capsaicin/TRPV1 promote cell proliferation but inhibit apoptosis under hyperoxic conditions. Next, the effects of hyperoxia on the proliferation and apoptosis of A549 cells were investigated. First, compared with the normal air group, the proliferation of A549 cells was significantly decreased in the hyperoxia group (Fig. 2A), consistent with a previous report on HILI (36). It is well established that capsaicin, a selective TRPV1 agonist (37,38), induces CGRP release from nerve endings (39). Additionally, TRPV1 channels exert a protective role in ischemia-reperfusion injury (19,30); however, the role of TRPV1 channels in HILI is unknown. Therefore, whether CGRP/CGRPR and capsaicin/TRPV1 exerted a protective effect in hyperoxia-induced alveolar cell injury was investigated. Indeed, CGRP and capsaicin enhanced cell proliferation of cells in both the normal air and hyperoxia groups in a dose-dependent manner (Fig. 2B and C). Based on these findings, 10 nM CGRP and 1 μM capsaicin were used in subsequent experiments. Moreover, hyperoxia significantly induced apoptosis in A549 cells, which was attenuated by CGRP and capsaicin (Fig. 2D). Taken together, CGRP/CGRPR and capsaicin/TRPV1 may play protective roles in hyperoxia-induced alveolar cell injury by promoting cell proliferation and inhibiting apoptosis.

CGRP promotes proliferation but inhibits apoptosis via a CGRPR/TRPV1 axis under hyperoxic conditions. Since CGRP/CGRPR and capsaicin/TRPV1 exerted protective effects in parallel, whether CGRP acted via a CGRPR/TRPV1 axis was next assessed. First, it was revealed that $CGRP_{8-37}$ (100 nM), a selective CGRPR inhibitor, inhibited CGRP-induced A549 cell proliferation with no toxic effects (Fig. 3A). Second, the selective TRPV1 channel blocker SB-705498 (10 μM) also attenuated CGRP-induced cell proliferation (Fig. 3B). Third, $CGRP_{8-37}$ and SB-705498 attenuated the inhibitory effect of CGRP on apoptosis, and they themselves had no significant effect on apoptosis (Fig. 3C and D). Therefore, CGRP may promote cell proliferation but inhibit apoptosis of A549 cells via a CGRPR/TRPV1 axis.

The CGRPR/TRPV1 axis affects transcription and protein expression levels of proliferation and apoptotic factors. Since Cyclin D1 and PCNA are critical factors for cell proliferation (40,41), while Bcl-2 and Bax are key targets of apoptosis (42,43), whether they were involved in the protective role of the CGRPR/TRPV1 axis in HILI was assessed. At the transcriptional level, compared with the normal air group, the mRNA expression levels of Cyclin D1 and PCNA in the hyperoxia group were significantly downregulated, and this was rescued by CGRP. However, $CGRP_{8-37}$ or SB-705498 significantly attenuated the CGRP-induced increase in Cyclin D1 and PCNA levels in the hyperoxic cells (Fig. 4A). Similarly, it was found that the mRNA expression levels of Bcl-2 were downregulated but Bax was upregulated in the hyperoxia group. However, CGRP increased the Bcl-2 expression, and this was reversed by either $CGRP_{8-37}$ or SB-705498 (Fig. 4B, left panel). By contrast, CGRP decreased the Bax expression, and this was reversed by either $CGRP_{8-37}$ or SB-705498 (Fig. 4B, right panel). Meanwhile, western blotting was performed to detect the expression of proliferation-related and apoptosis-related proteins after pretreatment with CGRP,

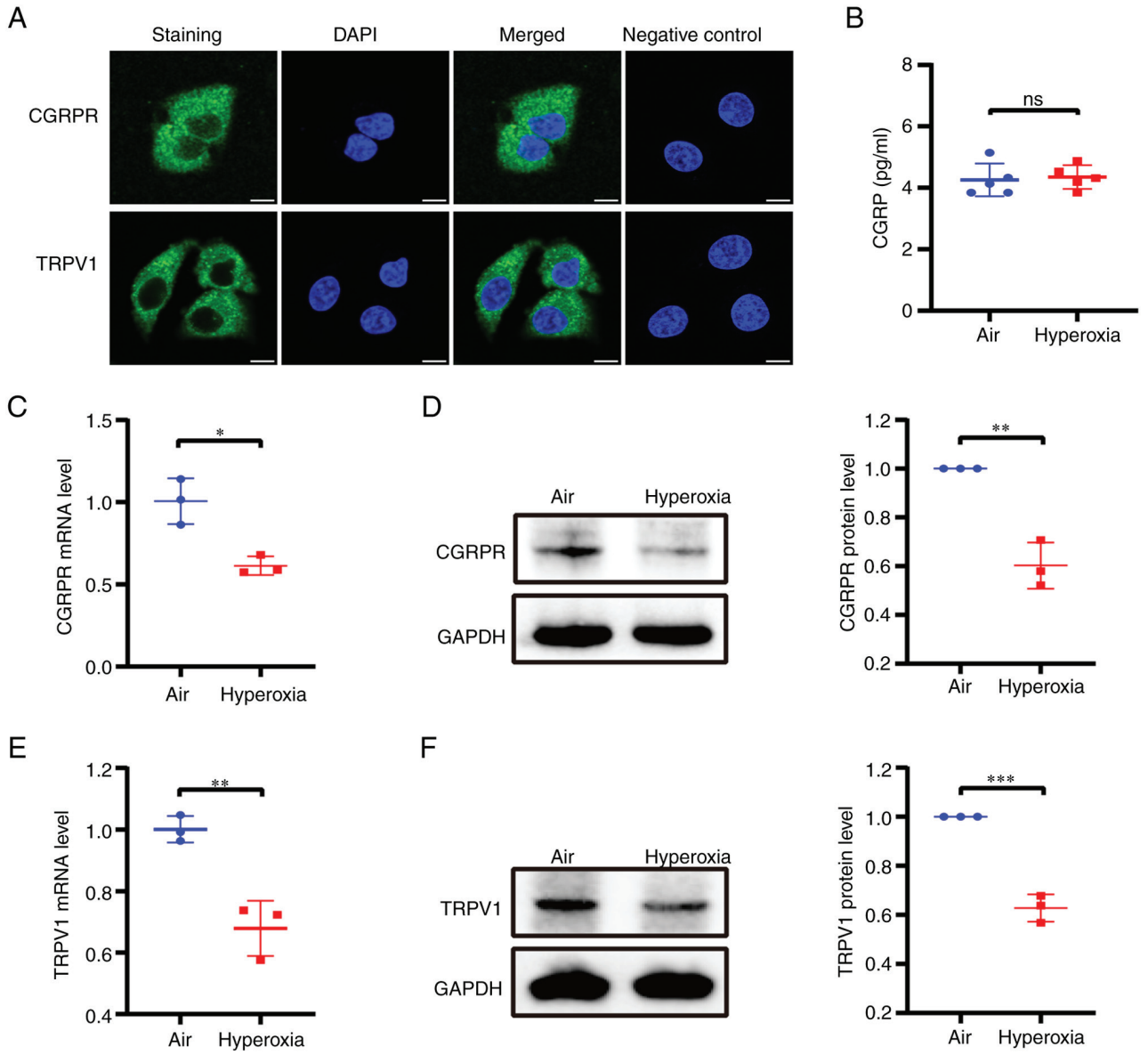

Figure 1. Release of CGRP and expression of CGRPR and TRPV1 in A549 cells under hyperoxic conditions. (A) Immunofluorescence staining for CGRPR and TRPV1 in A549 cells. Upper panel, CGRPR protein (green); lower panel, TRPV1 protein (green), the nuclei of the cells were counterstained with DAPI (blue). The negative control was not treated with the primary antibody. Scale bar, 10 μm. (B) Changes in CGRP release in A549 cells cultured under hyperoxic conditions. (C and D) qPCR and western blotting were used to determine the effects of hyperoxia on CGRPR expression in A549 cells. (E and F) qPCR and western blotting were used to determine the effects of hyperoxia on TRPV1 expression in A549 cells. Data are presented as the mean ± SD of at least three repeats. *P<0.05, **P<0.01 and ***P<0.001. CGRP, calcitonin gene-related peptide; CGRPR, CGRP receptor; TRPV1, transient receptor potential vanilloid 1; qPCR, quantitative PCR; ns, not significant.

$CGRP_{8-37}$ and SB-705498. The changes in these factors at the protein level reflected what was observed at the transcription level (Fig. 4C and D). Taken together, these data suggested that CGRP promotes proliferation but inhibits apoptosis of A549 cells via a CGRPR/TRPV1 axis.

Role of TRPV1 channels in CGRP-mediated cell proliferation and apoptosis in hyperoxia. First, lentiviral infection was used to knock down TRPV1 channels expression in A549 cells, and knockdown was confirmed at both the mRNA and protein levels (Fig. 5A and B). The shTRPV1-2 sequence exhibited the optimal result out of the three shRNAs used, and thus it was used for all subsequent experiments. ShTRPV1 significantly reduced CGRP-induced proliferation of A549 cells in hyperoxia (Fig. 5C). Similarly, CGRP had no inhibitory effect on apoptosis after shTRPV1 in hyperoxia (Fig. 5D). Finally, western blotting was used to analyze the effect of shTRPV1 on the protein expression levels of Cyclin D1, PCNA, Bcl-2 and Bax in hyperoxia. As demonstrated in Fig. 5E, shTRPV1 significantly attenuated the CGRP-induced upregulation of Cyclin D1, PCNA and Bcl-2 protein expression, and reversed the CGRP-induced downregulation of Bax expression. The results following the knockdown of TRPV1 in A549 cells were consistent with those of the selective TRPV1 blocker treatment (Fig. 4D). Therefore, these data confirmed the role of TRPV1 channels in CGRP-mediated proliferation and apoptosis of A549 cells in hyperoxia.

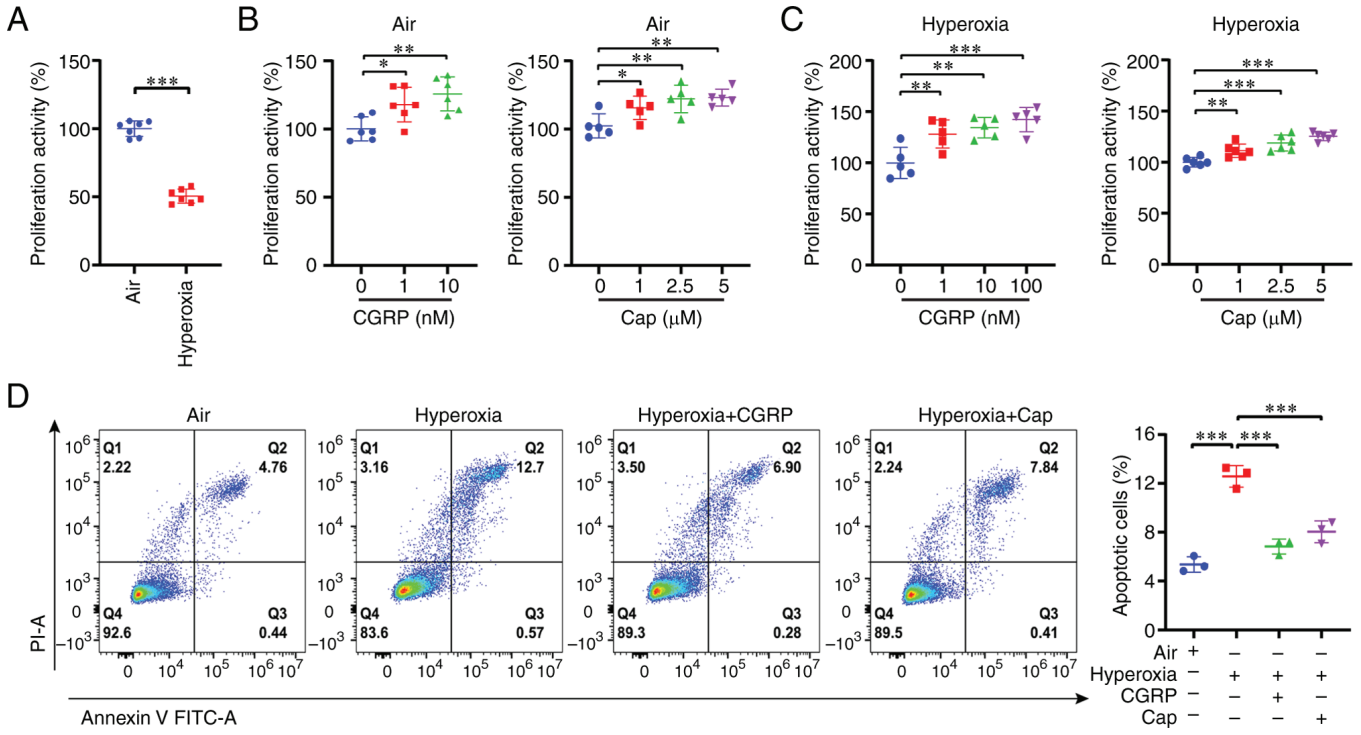

Figure 2. CGRP and cap promote cell proliferation but inhibit cell apoptosis in A549 cells grown under hyperoxic conditions. (A) Cell Counting Kit-8 assay revealed that hyperoxia inhibited A549 cell proliferation. (B) Different concentrations of CGRP (1 or 10 nM) and cap (1, 2.5, or 5 μM) promoted cell proliferation in the normal air group. (C) Different concentrations of CGRP (1, 10, or 100 nM) and cap (1, 2.5, or 5 μM) promoted cell proliferation under hyperoxia. (D) Flow cytometry revealed that hyperoxia promoted apoptosis of A549 cells, and both CGRP (10 nM) and cap (1 μM) reversed this. Data are presented as the mean ± SD of at least three repeats. *P<0.05, **P<0.01 and ***P<0.001. CGRP, calcitonin gene-related peptide; cap, capsaicin; PI, propidium iodine.

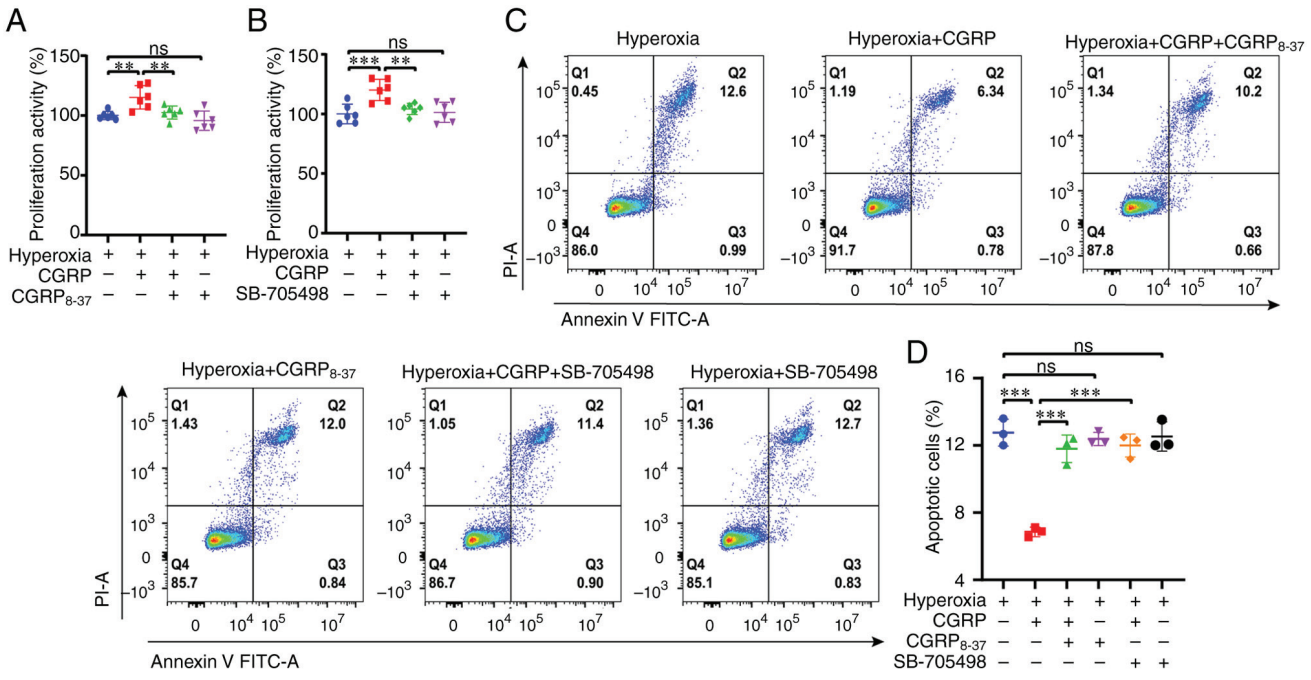

Figure 3. CGRP promotes A549 cell proliferation but inhibits apoptosis via the CGRPR/TRPV1 pathway under hyperoxic conditions. (A and B) Cell Counting Kit-8 assay revealed that 10 nM CGRP promoted the proliferation of A549 cells under hyperoxic conditions, and this was inhibited by both 100 nM $CGRP_{8-37}$ and 10 μM SB-705498. (C and D) Flow cytometry revealed that CGRP inhibited apoptosis of A549 cells cultured under hyperoxic conditions, and this was reversed by both $CGRP_{8-37}$ and SB-705498. Data are presented as the mean ± SD of at least three repeats. **P<0.01 and ***P<0.001. CGRP, calcitonin gene-related peptide; CGRPR, CGRP receptor; TRPV1, transient receptor potential vanilloid 1; ns, not significant; PI, propidium iodine.

CGRP induces Ca^{2+} entry via TRPV1 channels. Since TRPV1 channels are plasma membrane Ca^{2+}-permeable channels (32,44), whether CGRP protected against hyperoxia-induced alveolar cell injury via the TRPV1/Ca^{2+}

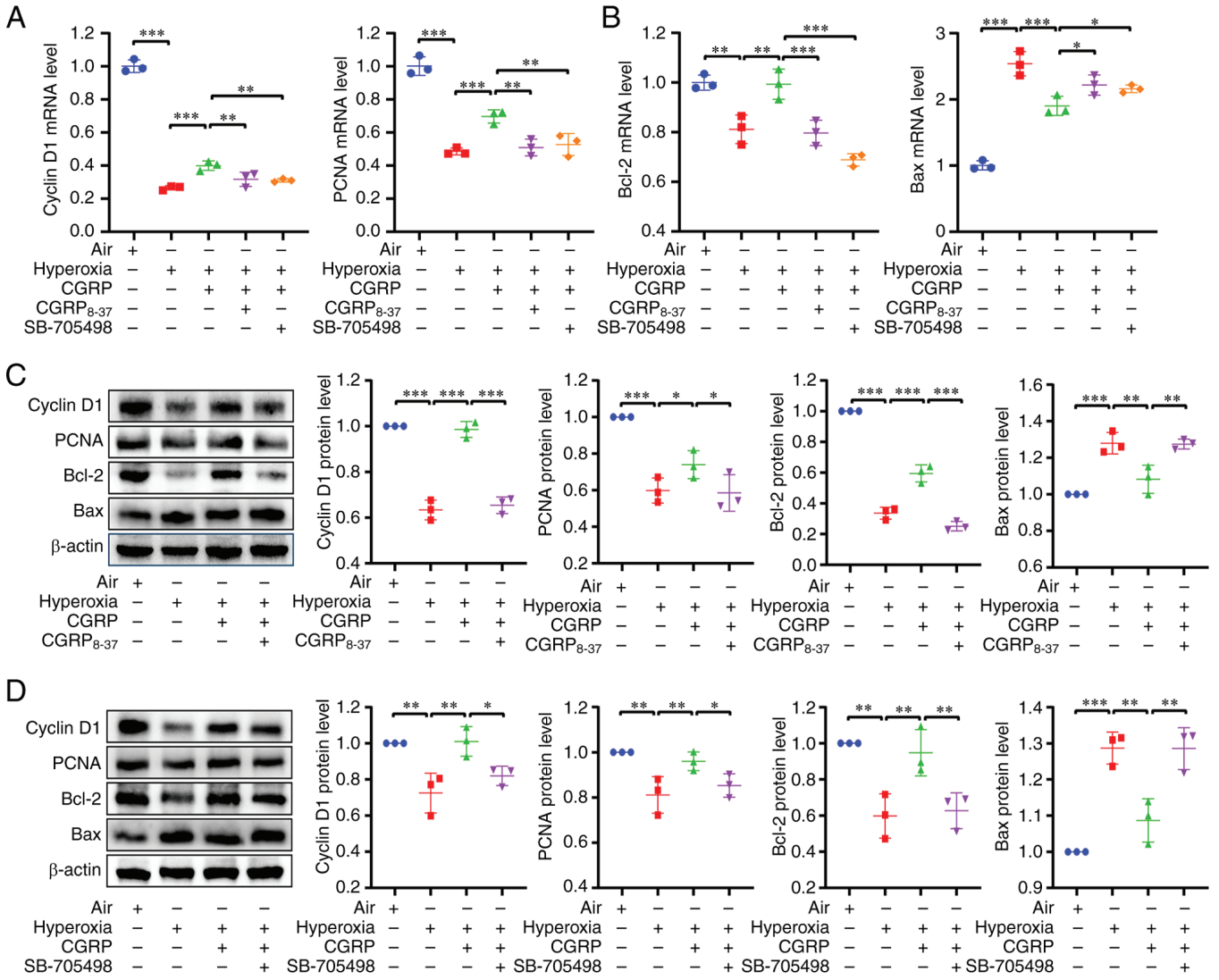

Figure 4. The CGRPR/TRPV1 axis regulates the mRNA and protein expression levels of proliferation and apoptosis factors in A549 cells under hyperoxic conditions. (A and B) quantitative PCR revealed the effects of 10 nM CGRP, 100 nM $CGRP_{8-37}$ and 10 μM SB-705498 on the expression of Cyclin D1, PCNA, Bcl-2 and Bax in A549 cells cultured under hyperoxic conditions. (C) Western blotting revealed the effects of CGRP and $CGRP_{8-37}$ on the expression levels of Cyclin D1, PCNA, Bcl-2 and Bax in A549 cells cultured under hyperoxic conditions. (D) Western blotting revealed the effects of CGRP and SB-705498 on the expression levels of Cyclin D1, PCNA, Bcl-2 and Bax in A549 cells cultured under hyperoxic conditions. Data are presented as the mean ± SD of at least three repeats. *P<0.05, **P<0.01 and ***P<0.001. CGRP, calcitonin gene-related peptide; CGRPR, CGRP receptor; TRPV1, transient receptor potential vanilloid 1; PCNA, proliferating cell nuclear antigen.

signaling pathway was examined. Patch-clamp and calcium imaging were performed using A549 cells. As demonstrated in the left panel of Fig. 6A, the membrane currents increased significantly with the addition of CGRP, while SB-705498 inhibited the CGRP-induced membrane currents. The middle panel of Fig. 6A shows a voltage-current diagram of the same cell, highlighting CGRP-induced membrane non-selective cation currents after SB-705498 treatment. Summary data on the right panel of Fig. 6A demonstrates that SB-705498 significantly inhibited CGRP-induced membrane currents. Subsequently, Ca^{2+} imaging experiments were performed in A549 cells. As revealed in Fig. 6B and D, CGRP induced a significant increase in intracellular Ca^{2+} signaling, which was attenuated by SB-705498. To further examine the importance of CGRP-mediated Ca^{2+} signaling in A549 cells, BAPTA-AM, a cell-permeable calcium chelator was used. It significantly attenuated the CGRP-induced intracellular Ca^{2+} signaling (Fig. 6C and E). In addition, it was found that BAPTA-AM (1 μM) attenuated the CGRP-induced proliferation of A549 cells in hyperoxia, while BAPTA-AM itself did not affect cell proliferation (Fig. 6F). By contrast, BAPTA-AM reversed the CGRP-induced decrease in apoptosis under hyperoxic conditions (Fig. 6G and H). These data suggested that CGRP protects against hyperoxia-induced alveolar cell injury via the TRPV1/Ca^{2+} signaling pathway.

The phospholipase C (PLC)/protein kinase C (PKC) pathway is involved in CGRP-mediated TRPV1/Ca^{2+} signaling. Activation of GPCR can stimulate TRPV1 channels to mediate inflammation via the PLC/PKC pathway (45-47). CGRPR acts as a GPCR, thus whether PLC/PKC was involved in the CGRPR/TRPV1/Ca^{2+} axis in A549 cells was examined. First, the role of PLC in CGRPR activation was examined. It was revealed that the selective PLC inhibitor U-73122

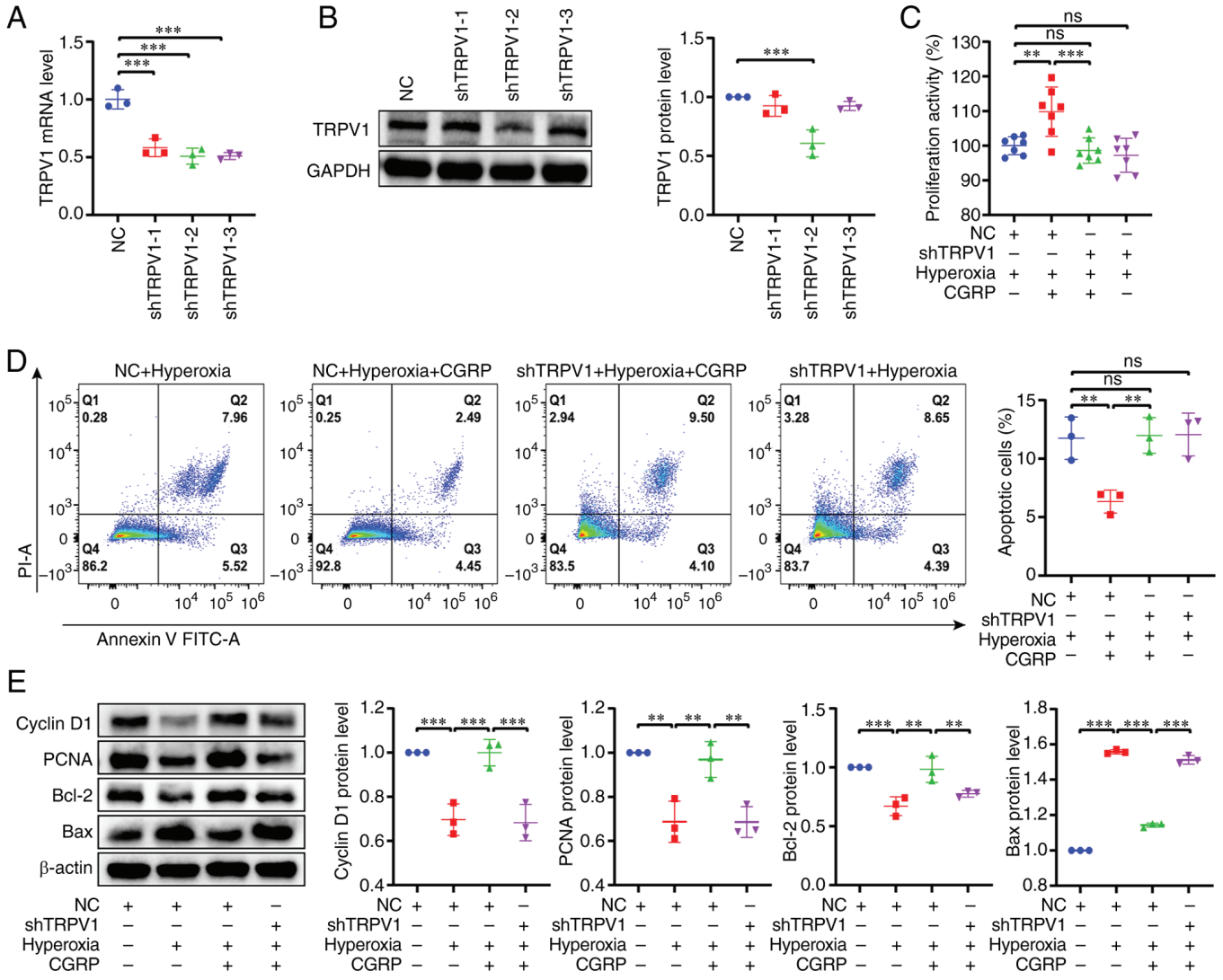

Figure 5. Knockdown of TRPV1 confirms the role of TRPV1 in CGRP-mediated cell proliferation and apoptosis of A549 cells cultured under hyperoxic conditions. (A and B) The mRNA and protein expression levels of TRPV1. For knockdown of TRPV1, three lentiviruses with different interference sequences were used. ShTRPV1-2 was used for subsequent experiments. (C) shTRPV1 attenuated the CGRP-induced increase in proliferation of A549 cells under hyperoxic conditions. (D) shTRPV1 attenuated the effect of CGRP-induced decrease in apoptosis of A549 cells under hyperoxic conditions. (E) Effects of CGRP on Cyclin D1, PCNA, Bcl-2 and Bax expression in A549 shTRPV1 cells cultured under hyperoxic conditions. Data are presented as the mean ± SD of at least three repeats. **P<0.01 and ***P<0.001. TRPV1, transient receptor potential vanilloid 1; CGRP, calcitonin gene-related peptide; m, messenger; sh, short hairpin; PCNA, proliferating cell nuclear antigen; NC, negative controls; ns, not significant; PI, propidium iodine.

(1 μM) reduced CGRP-induced Ca^{2+} signaling, whereas the inactive analog U-73343 did not reduce CGRP-induced Ca^{2+} signaling (Fig. 7A). In addition, whether PKC was involved in the activation of CGRPR/TRPV1 channels was assessed. CGRP-induced Ca^{2+} signaling was attenuated by the selective PKC inhibitor Go6976 (200 nM) (Fig. 7B). These results suggested that PLC/PKC is involved in activating CGRPR/TRPV1 channels.

CGRP/CGRPR regulates TRPV1/Ca^{2+} via the PLC/PKC pathway in hyperoxia. Further applying the PLC inhibitor U-73122 (1 μM) and PKC inhibitor Go6976 (200 nM), it was revealed that both inhibitors attenuated CGRP-induced cell proliferation in hyperoxia (Fig. 8A and B). In addition, both PLC and PKC inhibitors attenuated the CGRP-induced increase in Cyclin D1, PCNA and Bcl-2 protein expression, but reversed the CGRP-induced decrease in Bax expression (Fig. 8C-F). Therefore, these data suggested that CGRPR activates TRPV1 channels via the PLC/PKC pathway.

Discussion

In the present study, the protective role of CGRP in hyperoxia-induced human alveolar cell injury was verified, and the underlying molecular mechanisms were elucidated. The primary findings were as follows: i) Although hyperoxia treatment did not alter CGRP release from human alveolar cells, it significantly downregulated the mRNA and protein expression levels of CGRPR and TRPV1 channels; ii) CGRP promoted proliferation but inhibited apoptosis of human alveolar cells via the CGRPR/TRPV1/Ca^{2+} signaling axis in hyperoxia; iii) CGRP/CGRPR activated TRPV1 channels to induce Ca^{2+} entry via the PLC/PKC pathway; iv) CGRP protected against hyperoxia-induced human alveolar cell injury via regulation

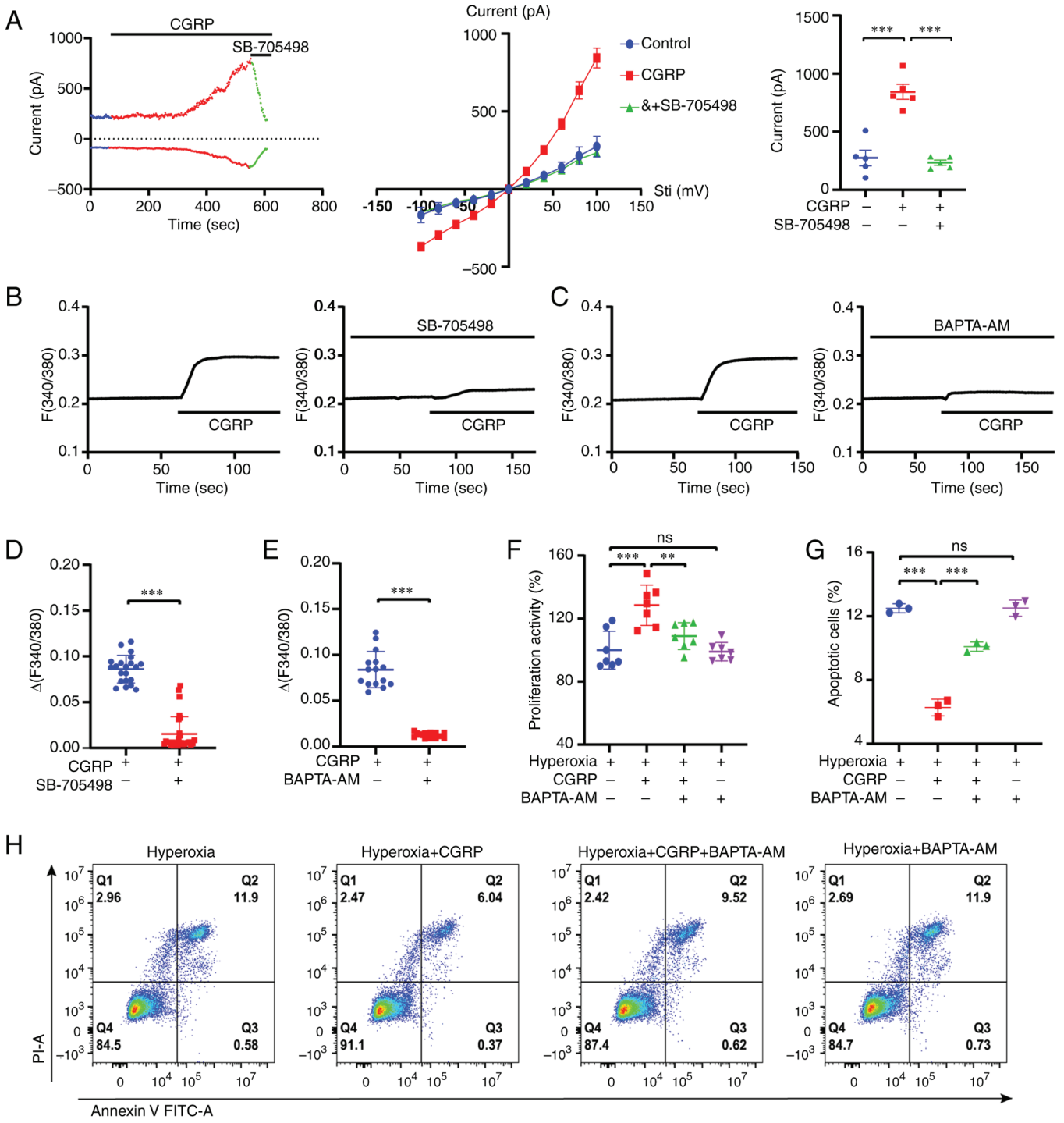

Figure 6. CGRP regulates Ca^{2+} entry into A549 cells via TRPV1 channels under hyperoxic conditions. (A) Left panel, membrane currents were increased by treatment with 100 nM CGRP and inhibited by 10 μM SB-705498. Middle panel, current-voltage curves in response to voltage stepping from -100 to +100 mV in the presence of 100 nM CGRP or combination of 10 μM SB-705498. Right panel, summary data of the membrane currents measured at 100 mV (n=5). (B and D) Time courses of 100 nM CGRP-induced intracellular Ca^{2+} signaling changes in the presence or the absence of 10 μM SB-705498, measured based on the Fura-2 ratio. Summary of the ΔFura-2 fluorescence ratio (the peak values) (n=20-30 cells per group). (C and E) Time courses of 100 nM CGRP-induced intracellular Ca^{2+} signaling changes in the presence or the absence of 1 μM BAPTA-AM, measured based on the Fura-2 ratio. Summary of the ΔFura-2 fluorescence ratio (the peak values) (n=15-20 cells per group). (F) Cell Counting Kit-8 assay revealed that 10 nM CGRP promoted A549 cell proliferation under hyperoxic conditions, which was inhibited by BAPTA-AM. (G and H) 10 nM CGRP inhibited A549 cell apoptosis under hyperoxic conditions, which was attenuated by BAPTA-AM. Data are presented as the mean ± SD of at least three repeats. **P<0.01 and ***P<0.001; CGRP, calcitonin gene-related peptide; TRPV1, transient receptor potential vanilloid 1; ns, not significant; PI, propidium iodine.

of proliferation and apoptotic factors Cyclin D1, PCNA, Bcl-2 and Bax.

It is well established that activation of TRPV1 channels at sensory nerve endings can induce the release of Ca^{2+}-dependent CGRP to exert biological effects by acting on CGRPR, indicating that the TRPV1/Ca^{2+} signaling pathway plays a key role in regulating CGRP release from sensory nerve endings (28,29). The present study

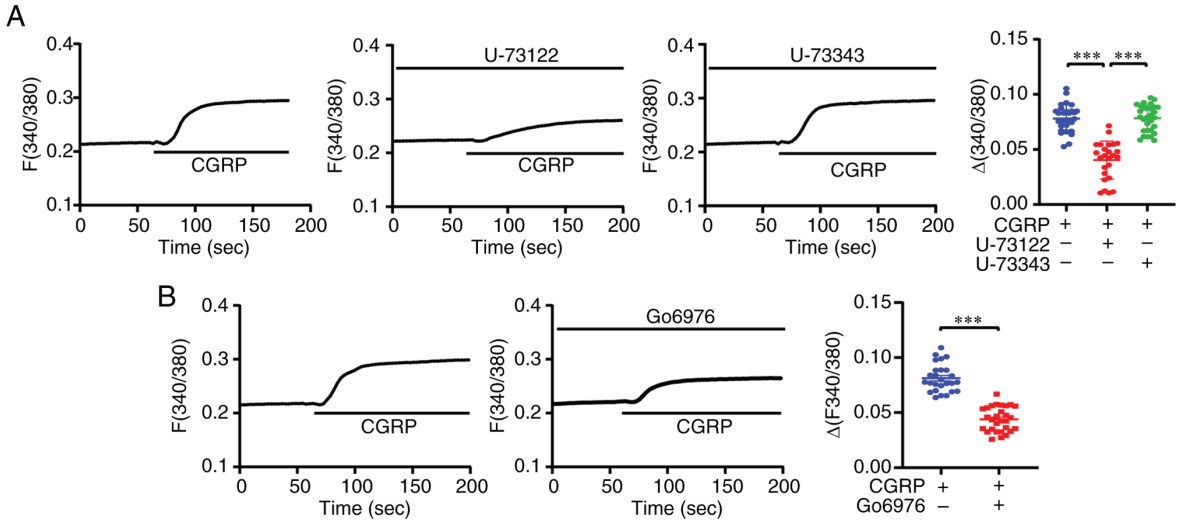

Figure 7. The PLC/PKC pathway is involved in CGRP-mediated TRPV1/Ca^{2+} signaling. (A) Left panel, time courses of 100 nM CGRP-induced intracellular Ca^{2+} signaling changes in the presence or the absence of 1 μM U-73122 or 1 μM U-73343, measured based on the Fura-2 ratio. Right panel, summary data of the ΔFura-2 fluorescence ratio. n=20-30 cells per group. (B) Left panel, time courses of CGRP-induced intracellular Ca^{2+} signaling changes in the presence or the absence of 200 nM Go6976, measured based on the Fura-2 ratio. Right panel, summary data of the ΔFura-2 fluorescence ratio. n=20-30 cells per group. Data are presented as the mean ± SD of at least three repeats. ***P<0.001. PLC, phospholipase C; PKC, protein kinase C; CGRP, calcitonin gene-related peptide; TRPV1, transient receptor potential vanilloid 1.

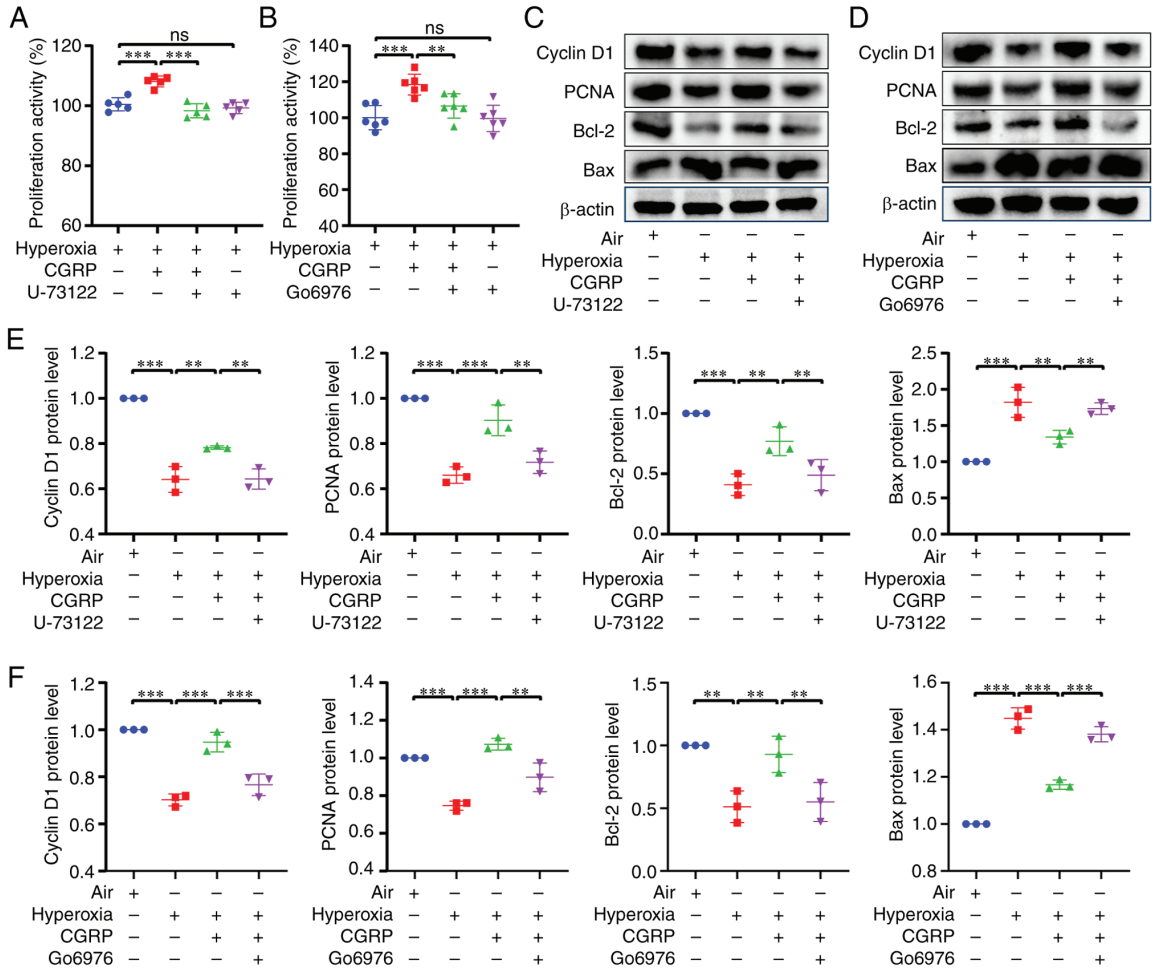

Figure 8. CGRP/CGRPR regulates TRPV1 via the PLC/PKC pathway in A549 cells cultured under hyperoxic conditions. (A and B) Cell Counting Kit-8 assay revealed that 10 nM CGRP promoted A549 cell proliferation under hyperoxic conditions, and this was inhibited by both 1 μM U-73122 and 200 nM Go6976. (C and D) Western blotting revealed CGRP increased the expression of Cyclin D1, PCNA and Bcl-2 and attenuated the expression of Bax in hyperoxia, whereas both U-73122 and Go6976 reversed the effects of CGRP. (E and F) The densitometric analysis diagram of the western blots. Data are presented as the mean ± SD of at least three repeats. **P<0.01 and ***P<0.001; CGRP, calcitonin gene-related peptide; CGRPR, CGRP receptor; TRPV1, transient receptor potential vanilloid 1; PLC, phospholipase C; PKC, protein kinase C; PCNA, proliferating cell nuclear antigen; ns, not significant.

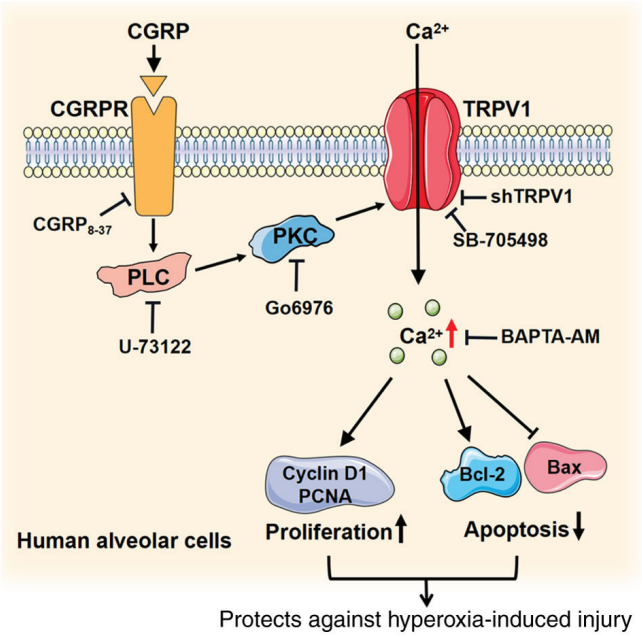

Figure 9. Diagram of the hypothesized CGRPR/TRPV1/Ca^{2+} signaling axis protecting human alveolar cells from hyperoxia-induced injury. CGRP/CGRPR activates TRPV1 channels via the PLC/PKC pathway to induce extracellular Ca^{2+} entry to promote cell proliferation and inhibit apoptosis under hyperoxia-induced injury, to ultimately protect against HILI. CGRP, calcitonin gene-related peptide; CGRPR, CGRP receptor; TRPV1, transient receptor potential vanilloid 1; PLC, phospholipase C; PKC, protein kinase C; HILI, hyperoxia-induced lung injury.

investigated whether CGRP acted inversely on TRPV1 channels to exert a protective effect against HILI from the perspective of CGRP. Previous studies have revealed that TRPV1 channels are functionally expressed in human bronchial epithelial cells, with increased expression in patients with asthma (48,49). However, there was no significant change in the expression of TRPV1 in pulmonary artery smooth muscle cells of rats under hypoxic conditions (50). Since the expression of TRPV1 under hyperoxia has not yet been reported to the best of the authors' knowledge, in the present study it was demonstrated for the first time that the expression of TRPV1 in human alveolar cells was downregulated under hyperoxic treatment. CGRPR expression is significantly downregulated in LPS-induced acute lung injury in rats (20). The expression of CGRPR under hyperoxic conditions was unknown however, in the present study, it was also demonstrated that hyperoxia downregulated CGRPR expression in A549 cells.

Although CGRP secretion from human alveolar cells was not altered by hyperoxia treatment compared with the control culture conditions, the exogenous addition of CGRP induced cell proliferation and inhibited cell apoptosis under hyperoxia, indicating that exogenous CGRP, but not endogenous CGRP, played a protective role in hyperoxia-induced human alveolar cell injury. Therefore, the protective role of exogenous CGRP and molecular mechanisms involved were further assessed. First, it was revealed that the promotion of cell proliferation by CGRP was attenuated by selective inhibitors of CGRPR and TRPV1. In addition, CGRP inhibited apoptosis in hyperoxia, but selective inhibitors for both CGRPR and TRPV1 reversed this inhibitory effect of CGRP on apoptosis. These results suggested that CGRPR/TRPV1 was involved in CGRP-mediated alveolar cell proliferation and apoptosis in hyperoxia. After applying selective inhibitors of CGRPR and TRPV1 channels or using shTRPV1 to knock down TRPV1 expression, the proliferation and apoptotic factors Cyclin D1, PCNA, Bcl-2 and Bax were assessed. Inhibition of CGRPR and TRPV1 channels reduced the protective effects of CGRP against hyperoxia-induced alveolar cell injury. Taken together, it was hypothesized that a CGRPR/TRPV1 axis plays a critical role in protecting alveolar cells under hyperoxic conditions.

It was also revealed that the TRPV1 agonist capsaicin promoted alveolar cell proliferation, but inhibited apoptosis under hyperoxia-induced injury, further highlighting the protective role of TRPV1. Since TRPV1 channels are plasma membrane Ca^{2+}-permeable channels (32,44), patch clamp and Ca^{2+} imaging were used to confirm that CGRP induced an increase in membrane non-selective currents and intracellular Ca^{2+} signaling, while SB-705498 inhibited these changes. The intracellular calcium chelator BAPTA-AM was also used to elucidate the role of TRPV1/Ca^{2+} signaling in CGRP/CGRPR protection against hyperoxia-induced alveolar cell injury.

CGRPR is a GPCR, its activation can regulate G_s/G_i to promote or inhibit adenylate cyclase to generate cAMP and can regulate the $G_{q/11}$-Ca^{2+} pathway (51). Since the CGRPR/cAMP pathway has been extensively studied (52-55), a focus was placed on the largely undefined CGRPR/Ca^{2+} pathway. Since activation of the $G_{q/11}$ protein promotes PLC activity (51), in the present study it was revealed that a PLC inhibitor reduced CGRP-induced intracellular Ca^{2+} signaling while attenuating the effects of CGRP-mediated protection against cell proliferation and apoptosis under hyperoxic conditions, suggesting that CGRP/CGRPR regulates $G_{q/11}$-PLC pathway. Due to PLC activating the PKC pathway, it was further confirmed that CGRP/CGRPR regulates PKC in alveolar cells. It was revealed that a PKC selective inhibitor attenuated the CGRP-induced increase in intracellular Ca^{2+} signaling in alveolar cells, while reversing the changes of CGRP-mediated proliferation and apoptotic factors Cyclin D1, PCNA, Bcl-2 and Bax. These data suggested that the PLC/PKC pathway plays a role in CGRP-mediated protection against hyperoxia-induced alveolar cell injury. However, the exact mechanisms of how the CGRPR/TRPV1/Ca^{2+} axis regulates proliferation-related and apoptosis-related factors need to be further elucidated.

Finally, the limitations of the present study will be discussed. Since the present study was performed at the *in vitro* cellular level, it lacks animal experiments or human *in vivo* experiments; thus, further *in vivo* experiments are required to verify the role of the identified CGRPR/TRPV1/Ca^{2+} axis. In addition, the human alveolar A549 cells were used to establish the cell model; not using primary AECII is also a potential limitation of the present study. The reasons for not using primary AECII are that primary human AECII are difficult to isolate and culture; and primary AECII isolated from rats have high background levels of apoptosis (56). Moreover, primary cultured AECII are prone to mutation and are unsuitable for transfection. However, the A549 cells, an AECII line, have similar

biological properties to AECII, are frequently used in studies on HILI, making them a valuable research subject for hyperoxia (57-61).

In conclusion, CGRP protected against hyperoxia-induced alveolar cell injury via a novel CGRPR/TRPV1/Ca^{2+} axis (Fig. 9). CGRP/CGRPR activated TRPV1 channels via the PLC/PKC pathway, inducing extracellular Ca^{2+} entry to promote cell proliferation but inhibit apoptosis following hyperoxic injury, ultimately protecting against HILI. Therefore, although activation of TRPV1 channels promotes Ca^{2+}-dependent CGRP release from sensory endings (28,29), in the present study it was revealed that exogenous CGRP could also inversely regulate the function of TRPV1 channels in alveolar cells. Importantly, the CGRPR/TRPV1/Ca^{2+} axis protected against hyperoxia-induced alveolar cell injury, highlighting a potential target for the management of HILI.

Since TRPV1 channels are located both on sensory endings to promote CGRP release and on alveolar cells to protect against hyperoxia-induced alveolar cell injury, the findings of the present study strongly suggested that capsaicin is a potential candidate to effectively prevent/treat HILI given its alveolar cell protective and anti-inflammatory effects (62-64), although this requires further study. Meanwhile, TRPV1 can be used as a drug development target in future studies to explore its role in the prevention and treatment of HILI.

Acknowledgements

Not applicable.

Funding

The present study was supported (grant no. 82273115) by research grants from the National Natural Science Foundation of China.

Availability of data and materials

The data generated in the present study may be requested from the corresponding author.

Authors' contributions

FX conceived the study and designed some experiments. HD designed all experiments, wrote and finalized the manuscript. JL performed most experiments and data analysis, and drafted the manuscript. HW, LW, FF and JW performed some experiments and revising the manuscript. All authors read and approved the final the manuscript. JL and FX confirm the authenticity of all the raw data.

Ethics approval and consent to participate

Not applicable.

Patient consent for publication

Not applicable.

Competing interests

The authors declare that they have no competing interests.

References

1. Dias-Freitas F, Metelo-Coimbra C and Roncon-Albuquerque R: Molecular mechanisms underlying hyperoxia acute lung injury. Respir Med 119: 23-28, 2016.
2. Kim MJ, Ryu JC, Kwon Y, Lee S, Bae YS, Yoon JH and Ryu JH: Dual Oxidase 2 in lung epithelia is essential for Hyperoxia-Induced acute lung injury in mice. Antioxid Redox Signal 21: 1803-1818, 2014.
3. Marseglia L, D'Angelo G, Granese R, Falsaperla R, Reiter RJ, Corsello G and Gitto E: Role of oxidative stress in neonatal respiratory distress syndrome. Free Radic Biol Med 142: 132-137, 2019.
4. Cannavò L, Perrone S, Viola V, Marseglia L, Di Rosa G and Gitto E: Oxidative stress and respiratory diseases in preterm newborns. Int J Mol Sci 22: 12504, 2021.
5. Nabhan AN, Brownfield DG, Harbury PB, Krasnow MA and Desai TJ: Single-cell wnt signaling niches maintain stemness of alveolar type 2 cells. Science 359: 1118-1123, 2018.
6. Pinho-Ribeiro FA, Baddal B, Haarsma R, O'Seaghdha M, Yang NJ, Blake KJ, Portley M, Verri WA, Dale JB, Wessels MR and Chiu IM: Blocking neuronal signaling to immune cells treats streptococcal invasive infection. Cell 173: 1083-1097.e22, 2018.
7. Bonner K, Pease JE, Corrigan CJ, Clark P and Kay AB: CCL17/thymus and activation-regulated chemokine induces calcitonin gene-related peptide in human airway epithelial cells through CCR4. J Allergy Clin Immunol 132: 942-950.e1-e3, 2013.
8. Bonner K, Kariyawasam HH, Ali FR, Clark P and Kay AB: Expression of functional receptor activity modifying protein 1 by airway epithelial cells with dysregulation in asthma. J Allergy Clin Immunol 126: 1277-1283.e3, 2010.
9. Li W, Hou L, Hua Z and Wang X: Interleukin-1β induces β-calcitonin gene-related peptide secretion in human type II alveolar epithelial cells. FASEB J 18: 1603-1605, 2004.
10. Wang W, Jia L, Wang T, Sun W, Wu S and Wang X: Endogenous calcitonin gene-related peptide protects human alveolar epithelial cells through protein kinase Cepsilon and heat shock protein. J Biol Chem 280: 20325-20330, 2005.
11. Russell FA, King R, Smillie SJ, Kodji X and Brain SD: Calcitonin Gene-related peptide: Physiology and pathophysiology. Physiol Rev 94: 1099-1142, 2014.
12. Edvinsson L: Calcitonin gene-related peptide (CGRP) is a key molecule released in acute migraine attacks-Successful translation of basic science to clinical practice. J Intern Med 292: 575-586, 2022.
13. Russo AF: Calcitonin Gene-related peptide (CGRP): A new target for migraine. Annu Rev Pharmacol Toxicol 55: 533-552, 2015.
14. Wu W, Feng B, Liu J, Li Y, Liao Y, Wang S, Tao S, Hu S, He W, Shu Q, *et al*: The CGRP/macrophage axis signal facilitates inflammation recovery in the intestine. Clin Immunol 245: 109154, 2022.
15. Yuan K, Zheng J, Shen X, Wu Y, Han Y, Jin X and Huang X: Sensory nerves promote corneal inflammation resolution via CGRP mediated transformation of macrophages to the M2 phenotype through the PI3K/AKT signaling pathway. Int Immunopharmacol 102: 108426, 2022.
16. Brain SD and Grant AD: Vascular actions of calcitonin Gene-related peptide and adrenomedullin. Physiol Rev 84: 903-934, 2004.
17. MaassenVanDenBrink A, Meijer J, Villalón CM and Ferrari MD: Wiping out CGRP: Potential cardiovascular risks. Trends Pharmacol Sci 37: 779-788, 2016.
18. Wurthmann S, Nägel S, Hadaschik E, Schlott S, Scheffler A, Kleinschnitz C and Holle D: Impaired wound healing in a migraine patient as a possible side effect of calcitonin gene-related peptide receptor antibody treatment: A case report. Cephalalgia 40: 1255-1260, 2020.
19. Zhao Q, Wang W, Wang R and Cheng Y: TRPV1 and neuropeptide receptor immunoreactivity and expression in the rat lung and brainstem after lung ischemia-reperfusion injury. J Surg Res 203: 183-192, 2016.

20. Yang W, Xv M, Yang WC, Wang N, Zhang XZ and Li WZ: Exogenous α-calcitonin gene-related peptide attenuates lipopolysaccharide-induced acute lung injury in rats. Mol Med Rep 12: 2181-2188, 2015.
21. Hong-Min F, Chun-Rong H, Rui Z, Li-Na S, Ya-Jun W and Li L: CGRP 8-37 enhances lipopolysaccharide-induced acute lung injury and regulating aquaporin 1 and 5 expressions in rats. J Physiol Biochem 73: 381-386, 2016.
22. Dang H, Yang L, Wang S, Fang F and Xu F: Calcitonin Gene-related peptide ameliorates Hyperoxia-induced lung injury in neonatal rats. Tohoku J Exp Med 227: 129-138, 2012.
23. Dang HX, Li J, Liu C, Fu Y, Zhou F, Tang L, Li L and Xu F: CGRP attenuates hyperoxia-induced oxidative stress-related injury to alveolar epithelial type II cells via the activation of the Sonic hedgehog pathway. Int J Mol Med 40: 209-216, 2017.
24. Fu H, Zhang T, Huang R, Yang Z, Liu C, Li M, Fang F and Xu F: Calcitonin gene-related peptide protects type II alveolar epithelial cells from hyperoxia-induced DNA damage and cell death. Exp Ther Med 13: 1279-1284, 2017.
25. Bai Y, Fang F, Jiang J and Xu F: Extrinsic calcitonin Gene-related peptide inhibits hyperoxia-induced alveolar epithelial type II cells apoptosis, oxidative stress, and reactive oxygen species (ROS) production by enhancing Notch 1 and Homocysteine-Induced endoplasmic reticulum protein (HERP) expression. Med Sci Monit 23: 5774-5782, 2017.
26. Negri S, Faris P, Rosti V, Antognazza MR, Lodola F and Moccia F: Endothelial TRPV1 as an emerging molecular target to promote therapeutic angiogenesis. Cells 9: 1341, 2020.
27. Caterina MJ, Schumacher MA, Tominaga M, Rosen TA, Levine JD and Julius D: The capsaicin receptor: A heat-activated ion channel in the pain pathway. Nature 389: 816-824, 1997.
28. Riera CE, Huising MO, Follett P, Leblanc M, Halloran J, Van Andel R, de Magalhaes Filho CD, Merkwirth C and Dillin A: TRPV1 pain receptors regulate longevity and metabolism by neuropeptide signaling. Cell 157: 1023-1036, 2014.
29. Nakanishi M, Hata K, Nagayama T, Sakurai T, Nishisho T, Wakabayashi H, Hiraga T, Ebisu S and Yoneda T: Acid activation of Trpv1 leads to an Up-Regulation of calcitonin Gene-related peptide expression in dorsal root ganglion neurons via the CaMK-CREB cascade: A potential mechanism of inflammatory pain. Mol Biol Cell 21: 2568-2577, 2010.
30. Li X, Xu Y, Cheng Y and Wang R: α7 nicotinic acetylcholine receptor contributes to the alleviation of lung ischemia-reperfusion injury by transient receptor potential vanilloid type 1 stimulation. J Surg Res 230: 164-174, 2018.
31. Lu X, Wang C, Wu D, Zhang C, Xiao C and Xu F: Quantitative proteomics reveals the mechanisms of hydrogen-conferred protection against hyperoxia-induced injury in type II alveolar epithelial cells. Exp Lung Res 44: 464-475, 2018.
32. Gao N, Yang F, Chen S, Wan H, Zhao X and Dong H: The role of TRPV1 ion channels in the suppression of gastric cancer development. J Exp Clin Cancer Res 39: 206, 2020.
33. Zhou J, Jiang Y, Chen H, Wu Y and Zhang L: Tanshinone I attenuates the malignant biological properties of ovarian cancer by inducing apoptosis and autophagy via the inactivation of PI3K/AKT/mTOR pathway. Cell Prolif 53: e12739, 2020.
34. Chen X, Lu W, Lu C, Zhang L, Xu F and Dong H: The CaSR/TRPV4 coupling mediates pro-inflammatory macrophage function. Acta Physiol (Oxf) 237: e13926, 2023.
35. Livak KJ and Schmittgen TD: Analysis of relative gene expression data using real-time quantitative PCR and the 2(-Delta Delta C(T)) method. Methods 25: 402-408, 2001.
36. Li Z, Fang F and Xu F: Effects of different states of oxidative stress on fetal rat alveolar type II epithelial cells *in vitro* and ROS-induced changes in wnt signaling pathway expression. Mol Med Rep 7: 1528-1532, 2013.
37. Jordt SE and Julius D: Molecular basis for species-specific sensitivity to 'hot' chili peppers. Cell 108: 421-430, 2002.
38. Zhu SL, Wang ML, He YT, Guo SW, Li TT, Peng WJ and Luo D: Capsaicin ameliorates intermittent high glucose-mediated endothelial senescence via the TRPV1/SIRT1 pathway. Phytomedicine 100: 154081, 2022.
39. Lin YT, Yu Z, Tsai SC, Hsu PH and Chen JC: Neuropeptide FF receptor 2 inhibits capsaicin-induced CGRP upregulation in mouse trigeminal ganglion. J Headache Pain 21: 87, 2020.
40. Shi L, Zhang S, Huang Z, Hu F, Zhang T, Wei M, Bai Q, Lu B and Ji L: Baicalin promotes liver regeneration after acetaminophen-induced liver injury by inducing NLRP3 inflammasome activation. Free Radic Biol Med 160: 163-177, 2020.
41. Liao S, Chen H, Liu M, Gan L, Li C, Zhang W, Lv L and Mei Z: Aquaporin 9 inhibits growth and metastasis of hepatocellular carcinoma cells via Wnt/β-catenin pathway. Aging (Albany NY) 12: 1527-1544, 2020.
42. Fu YP, Yuan H, Xu Y, Liu RM, Luo Y and Xiao JH: Protective effects of Ligularia fischeri root extracts against ulcerative colitis in mice through activation of Bcl-2/Bax signalings. Phytomedicine 99: 154006, 2022.
43. Zhang Y, Yang X, Ge X and Zhang F: Puerarin attenuates neurological deficits via Bcl-2/Bax/cleaved caspase-3 and Sirt3/SOD2 apoptotic pathways in subarachnoid hemorrhage mice. Biomed Pharmacother 109: 726-733, 2019.
44. Yuan J, Liu H, Zhang H, Wang T, Zheng Q and Li Z: Controlled activation of TRPV1 channels on microglia to boost their autophagy for clearance of Alpha-Synuclein and enhance therapy of Parkinson's disease. Adv Mater 34: 2108435, 2022.
45. Than JYXL, Li L, Hasan R and Zhang X: Excitation and modulation of TRPA1, TRPV1, and TRPM8 Channel-expressing sensory neurons by the pruritogen chloroquine. J Biol Chem 288: 12818-12827, 2013.
46. Minke B and Pak WL: The light-activated TRP channel: The founding member of the TRP channel superfamily. J Neurogenet 36: 55-64, 2022.
47. Kumar R, Hazan A, Geron M, Steinberg R, Livni L, Matzner H and Priel A: Activation of transient receptor potential vanilloid 1 by lipoxygenase metabolites depends on PKC phosphorylation. FASEB J 31: 1238-1247, 2017.
48. McGarvey LP, Butler CA, Stokesberry S, Polley L, McQuaid S, Abdullah H, Ashraf S, McGahon MK, Curtis TM, Arron J, *et al*: Increased expression of bronchial epithelial transient receptor potential vanilloid 1 channels in patients with severe asthma. J Allergy Clin Immunol 133: 704-712.e4, 2014.
49. Grace MS, Baxter M, Dubuis E, Birrell MA and Belvisi MG: Transient receptor potential (TRP) channels in the airway: Role in airway disease. Br J Pharmacol 171: 2593-2607, 2014.
50. Parpaite T, Cardouat G, Mauroux M, Gillibert-Duplantier J, Robillard P, Quignard JF, Marthan R, Savineau JP and Ducret T: Effect of hypoxia on TRPV1 and TRPV4 channels in rat pulmonary arterial smooth muscle cells. Pflugers Arch 468: 111-130, 2016.
51. Cottrell GS: CGRP receptor signalling pathways. In: Calcitonin Gene-Related peptide (CGRP) mechanisms. vol. 255 Brain SD and Geppetti P (eds.) Springer International Publishing, Cham, pp37-64, 2018.
52. Zhang Y, Xu J, Ruan YC, Yu MK, O'Laughlin M, Wise H, Chen D, Tian L, Shi D, Wang J, *et al*: Implant-derived magnesium induces local neuronal production of CGRP to improve bone-fracture healing in rats. Nat Med 22: 1160-1169, 2016.
53. Do TP, Deligianni C, Amirguliyev S, Snellman J, Lopez CL, Al-Karagholi MA, Guo S and Ashina M: Second messenger signalling bypasses CGRP receptor blockade to provoke migraine attacks in humans. Brain 146: 5224-5234, 2023.
54. Villa I, Mrak E, Rubinacci A, Ravasi F and Guidobono F: CGRP inhibits osteoprotegerin production in human osteoblast-like cells via cAMP/PKA-dependent pathway. Am J Physiol Cell Physiol 291: C529-C537, 2006.
55. Hartopo AB, Emoto N, Vignon-Zellweger N, Suzuki Y, Yagi K, Nakayama K and Hirata K: Endothelin-converting Enzyme-1 gene ablation attenuates pulmonary fibrosis via CGRP-cAMP/EPAC1 pathway. Am J Respir Cell Mol Biol 48: 465-476, 2013.
56. Geiser T, Ishigaki M, Van Leer C, Matthay MA and Broaddus VC: H(2)O(2) inhibits alveolar epithelial wound repair in vitro by induction of apoptosis. Am J Physiol Lung Cell Mol Physiol 287: L448-L453, 2004.
57. Bao T, Liu X, Hu J, Ma M, Li J, Cao L, Yu B, Cheng H, Zhao S and Tian Z: Recruitment of PVT1 enhances YTHDC1-mediated m6A modification of IL-33 in Hyperoxia-induced lung injury during bronchopulmonary dysplasia. Inflammation: Nov 2, 2023 doi: 10.1007/s10753-023-01923-1 (Epub ahead of print).
58. Yang M, Chen Y, Huang X, Shen F and Meng Y: ETS1 Ameliorates Hyperoxia-Induced bronchopulmonary dysplasia in mice by activating Nrf2/HO-1 mediated ferroptosis. Lung 201: 425-441, 2023.
59. Zhang X, Chu X, Gong X, Zhou H and Cai C: The expression of miR-125b in Nrf2-silenced A549 cells exposed to hyperoxia and its relationship with apoptosis. J Cell Mol Med 24: 965-972, 2020.
60. He F, Wang QF, Li L, Yu C, Liu CZ, Wei WC, Chen LP and Li HY: Melatonin protects against hyperoxia-induced apoptosis in alveolar epithelial type II cells by activating the MT2/PI3K/AKT/ETS1 signaling pathway. Lung 201: 225-234, 2023.

61. Wang X, Huo R, Liang Z, Xu C, Chen T, Lin J, Li L, Lin W, Pan B, Fu X and Chen S: Simvastatin Inhibits NLRP3 inflammasome activation and ameliorates lung injury in Hyperoxia-Induced bronchopulmonary dysplasia via the KLF2-Mediated mechanism. Oxid Med Cell Longev 2022: 8336070, 2022.
62. Wan H, Chen XY, Zhang F, Chen J, Chu F, Sellers ZM, Xu F and Dong H: Capsaicin inhibits intestinal Cl-secretion and promotes Na+ absorption by blocking TRPV4 channels in healthy and colitic mice. J Biol Chem 298: 101847, 2022.
63. Chen YS, Lian YZ, Chen WC, Chang CC, Tinkov AA, Skalny AV and Chao JCJ: Lycium barbarum polysaccharides and capsaicin inhibit oxidative stress, inflammatory responses, and pain signaling in rats with dextran sulfate sodium-induced colitis. Int J Mol Sci 23: 2423, 2022.
64. Zhang Q, Luo P, Xia F, Tang H, Chen J, Zhang J, Liu D, Zhu Y, Liu Y, Gu L, *et al*: Capsaicin ameliorates inflammation in a TRPV1-independent mechanism by inhibiting PKM2-LDHA-mediated Warburg effect in sepsis. Cell Chem Biol 29: 1248-1259.e6, 2022.